J. M., Boots, H. A., & Tijhuis, M. W. (1981) *J. Org. Chem. 46*, 3273-3283.
Ottenheijm, H. C. J., van den Broek, L. A. G. M., Ballesta, J. P. G., & Zylicz, Z. (1986) *Prog. Med. Chem. 23*, 219-268.
Perez-Gosalbez, M., Leon Rivera, G., & Ballesta, J. P. G. (1983) *Biochem. Biophys. Res. Commun. 113*, 941-947.
Pestka, S. (1969) *Proc. Natl. Acad. Sci. U.S.A. 64*, 709-714.
Rheinberger, H. J., Geigenmüller, U., Gnirke, A., Hausner, T.-P., Remme, J., Saruyama, J., & Nierhaus, K. (1990) in *The Ribosome. Structure, Function & Evolution* (Hill, W. E., Dahlberg, A., Garrett, R. A., Moore, P. B., Schlessinger, D., & Warner, J. R., Eds.) pp 318-330, American Society for Microbiology, Washington, DC.
Smith, A. E. (1973) *Eur. J. Biochem. 33*, 301-313.
Staehelin, T., & Maglott, D. R. (1971) *Methods Enzymol. 20*, 449-456.
Szer, W., & Kurylo-Borowska, Z. (1970) *Biochim. Biophys. Acta 224*, 477-486.
Szer, W., & Kurylo-Borowska, Z. (1972) *Biochim. Biophys. Acta 259*, 357-368.
Tejedor, F., & Ballesta, J. P. G. (1982) *Anal. Biochem. 127*, 143-149.
van den Broek, L. A. G. M., Liskamp, R. M. J., Colstee, J. H., Lelieveld, P., Remacha, M., Vazquez, D., Ballesta, J. P. G., & Ottenheijm, H. C. J. (1987) *J. Med. Chem. 30*, 325-333.
van den Broek, L. A. G. M., Lazaro, E., Zylicz, Z., Fennis, P. J., Missler, F. A. N., Leleiveld, P., Garzotto, M., Wagener, D. J. T., Ballesta, J. P. G., & Ottenheijm, H. C. J. (1989) *J. Med. Chem. 32*, 2002-2015.
Vazquez, D. (1979) *Mol. Biol. Biochem. Biophys. 30*, 1-312.
Zylicz, Z. (1988) Ph.D. Thesis, University of Nijmegen, The Netherlands.

Motion of Aromatic Side Chains, Picosecond Fluorescence, and Internal Energy Transfer in *Escherichia coli* Thioredoxin Studied by Site-Directed Mutagenesis, Time-Resolved Fluorescence Spectroscopy, and Molecular Dynamics Simulations†

Arne Elofsson,*,‡ Rudolf Rigler,*,‡ Lennart Nilsson,‡ Johnny Roslund,§ Günter Krause,∥ and Arne Holmgren∥
Departments of Medical Biophysics and Physiological Chemistry, Karolinska Institutet, Box 60400, S-10401 Stockholm, Sweden, and Max-lab, University of Lund, Lund, Sweden
Received January 22, 1991; Revised Manuscript Received May 23, 1991

ABSTRACT: We have determined the picosecond fluorescence of the four aromatic amino acid residues (W28, W31, Y49, and Y70) in wild-type *Escherichia coli* thioredoxin (wt Trx) and a mutant Trx with W31 replaced by phenylalanine, Trx-W28-W31F. The internal motions of the four aromatic side chains were also analyzed. We examined the possibility of using internal energy transfer from tyrosine to tryptophan as a measure of long-range distances. The major features of the lifetime distribution of tryptophan fluorescence were unchanged in the W31F mutation, indicating that the environment of W28 is similar in both wt Trx and Trx-W28-W31F. However, the mutation of W31F changed the mobility of W28, situated close to the active-site disulfide/dithiol, but not the mobility of two tyrosines, Y49 and Y70, situated on the other side of the molecule. The mobility of the two tyrosine residues increased upon reduction of the active-site disulfide, indicating a looser structure with reduction. This increased motion could also be seen from molecular dynamics simulations. The change in energy transfer rates, as judged by tyrosine fluorescence lifetimes, was in agreement with energy transfer rates calculated from the molecular dynamics simulations. The anisotropy of tryptophan and tyrosine fluorescence could be separated in three parts: (I) overall rotation of the protein (10^{-9} s), (II) internal mobility of side chains (10^{-10} s), and (III) a very fast relaxation (10^{-12} s). We can only experimentally detect this very fast relaxation when the internal motion is not present.

To understand the action of enzymes, it is important to study their dynamics. From molecular dynamics simulations, it is known that proteins vibrate around an average structure, but during catalysis by an enzyme it is often necessary that larger rearrangements occur. Thioredoxin from *Escherichia coli* is a suitable model protein for studying side-chain rearrangements since it contains a redox-active disulfide in the active site.

All thioredoxins have a common active disulfide ring W31-C-G-P-C-K36 (Holmgren, 1985). *E. coli* Trx[1] contains 108 amino acid residues, a single disulfide bridge (C32–C35), two tyrosines (Y49, Y70), and two tryptophans (W28, W31). The molecule is globular and has five β-pleated sheet strands and four α-helixes. The active center disulfide bridge is located in a loop positioned at the C-terminal end of a β-strand (β_2) and followed by an α-helix (α_2). The active center is close to Y70 and both the tryptophans (Figure 1). The disulfide bridge involved in the redox action of the thioredoxin is exposed in the protein.

† This work was supported by grants from the Swedish Board for Technical Development, the Swedish Natural Science Council, the Swedish Medical Research Council (13X-3529), and the Karolinska Institute.
* To whom correspondence should be addressed.
‡ Department of Medical Biophysics, Karolinska Institutet.
§ Max-lab, University of Lund.
∥ Department of Physiological Chemistry, Karolinska Institutet.

[1] Abbreviations: Trx, Thioredoxin; wt, wild-type; Trx-W28-W31F, Trx with tryptophan 28 exchanged for phenylalanine; Trx-S_2, oxidized Trx; Trx-$(SH)_2$, reduced Trx; MD, molecular dynamics; DTT, dithiothreitol.

0006-2960/91/0430-9648$02.50/0

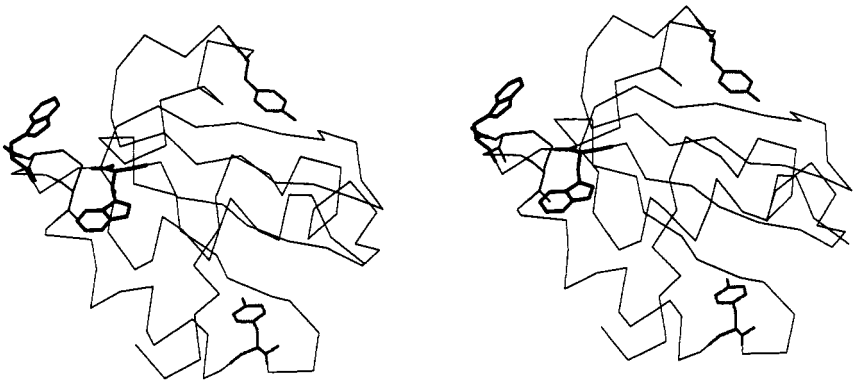

FIGURE 1: Stereodrawing of thioredoxin X-ray structure. Tryptophan residues are shown by thick lines, tyrosine residues by dashed lines, and the cystine disulfide bridge by middle sized lines and CA backbone by a thin line.

The structure of wt Trx is extremely well characterized (Holmgren, 1985). X-ray crystallography of the oxidized form (Trx-S_2) has been refined to a resolution of 1.7 Å (Katti et al., 1990). Recently, the structure of the reduced form [Trx-$(SH)_2$] was solved by 2D ^{1}H NMR (Dyson et al., 1990). Since it is a small protein, it is well suited for molecular dynamics simulations.

Since the two tryptophan residues in wt Trx are located close to the active site (C32, C35), tryptophan fluorescence provides an extremely sensitive probe for monitoring structural changes during the catalytic oxidation–reduction cycle.

The quantum yield of tryptophan fluorescence in Trx-S_2 is extremely low due to both dynamic and static quenching (Merola et al., 1989). Upon reduction of the disulfide bridge in Trx-S_2, a 3-fold increase in fluorescence is observed (Holmgren, 1972). Chemical modification studies (Holmgren, 1981) and comparison of yeast and calf thymus thioredoxins (Merola et al., 1989) attribute this rise in fluorescence to W28. Variants of *E. coli* Trx with W31 replaced by alanine, histidine, phenylalanine, and tyrosine have been made by site-directed mutagenesis and confirmed the importance of W28 as being responsible for the fluorescence increase upon reduction of Trx-S_2 (Krause & Holmgren, 1991).

Reduction of the disulfide in Trx-S_2 results in a local conformational change around the active site as seen by 2D NMR (Dyson et al., 1990). In this paper, we have studied mobility changes of the fluorescent residues W28 and W31, which are near the active site, plus the more remote residues Y49 and Y70.

The fluorescence decay of the two tryptophans in wt Trx has been previously studied by time-resolved fluorescence spectroscopy (Merola et al., 1989), showing the existence of several tryptophan conformations. We have complemented this investigation with studies on the tyrosine motions, using a mutant with W31 exchanged for phenylalanine and measurements of the energy transfer from tyrosine to tryptophan. Side-chain mobilities and energy transfer rates were calculated from molecular dynamics simulations and compared with experimentally obtained values.

A complete investigation using several MD simulations and a comparison with the recently obtained NMR structure (Dyson et al., 1990) will be published elsewhere.

Materials and Methods

Theory of Energy Transfer

Energy transfer from a donor to an acceptor was described by Förster (Förster, 1948). The transfer is a dipole–dipole interaction with a transfer rate k_τ dependent on an orientation factor κ, the distance between the donor and acceptor, r, and the lifetime of the donor in absence of the acceptor τ_d, as follows:

$$k_\tau = C\kappa^2 r^{-6} \tau_d^{-1} \tag{1}$$

where C is a constant depending on the spectral properties of the fluorophores involved (Förster, 1948):

$$C = \frac{9000(\ln 10)\phi_d}{128\pi^5 n^4 N} \int_0^\infty \frac{F_d(\bar{\nu})\epsilon_a(\bar{\nu})}{\bar{\nu}^4}\, d\bar{\nu} \tag{2}$$

Here ϕ_d is the quantum yield of the donor in the absence of acceptor, n is the refractive index of the medium, N is Avogadro's number, r is the distance between the donor and acceptor, $F_d(\bar{\nu})$ is the corrected fluorescence intensity of the donor in the wave number range $\bar{\nu}$ to $\bar{\nu} + d\bar{\nu}$ with the total intensity normalized to unity, and $\epsilon_a(\bar{\nu})$ is the extinction coefficient of the acceptor at $\bar{\nu}$.

Absorption spectra were recorded with a Varian Cary 118 UV–visible spectrophotometer. Fluorescence spectra were obtained on a Shimadzu RF-540 fluorometer and were not corrected for monochromator and photomultiplier efficiency. These measurements gave a constant, C, equal to 1.6×10^7 m^6 for tyrosine to tryptophan transfer.

κ is a factor describing the relative orientation of the transition dipoles of the donor and the acceptor given by

$$\kappa = (\hat{\mu}_d \cdot \hat{\mu}_a) - 3(\hat{\mu}_d \cdot \hat{\mathbf{R}})(\hat{\mu}_a \cdot \hat{\mathbf{R}}) \tag{3}$$

where $\hat{\mu}_D$ and $\hat{\mu}_a$ are the transition moment vectors of the donor and the acceptor, respectively, and $\hat{\mathbf{R}}$ is the vector between the donor and acceptor, all normalized to unity. κ^2 is often set equal to $^2/_3$, which is the mean value obtained if the donor and acceptor have unrestricted mobility. The Förster distance (R_0) is the distance between the donor and acceptor, where the probability for transfer is equal to the probability for natural decay, this occurs when

$$k_\tau = 1/\tau_d \tag{4}$$

The measured value of the constant C corresponds to an R_0 of 15 Å, in agreement with earlier studies (Lakowicz, 1983). The donor and acceptor might have strongly restricted motion in proteins and therefore a value of $^2/_3$ need not always be correct; however, since k_τ varies with $1/r^6$, a small error in κ^2 would only give rise to a very small error in the distance. This might make it meaningful to set κ^2 equal to a constant determined from eq 3 if the structure is known or to $^2/_3$ if not.

Transition Moments in Aromatics

The absorption in tryptophan is along two axes, L_a and L_b. L_a is situated −38° from the longest axis in tryptophan, while L_b is approximately perpendicular to L_a (Yamamoto & Ta-

naka, 1972; Ruggiero et al., 1990). The angle between L_a and L_b varies with excitation and emission wavelength. There is rapid nonmotional relaxation between L_a and L_b giving a very fast (1.6 ps) nonexponential decay of the anisotropy of tryptophan fluorescence. At longer excitation and emission wavelengths, most of the fluorescence occurs from L_a, but at no wavelength is the contribution from L_b negligible. We used L_a for rotational calculations from the MD simulation as it is the dominant transition moment for emission above 345 nm (Ruggiero et al., 1990) as measured in the present experiments.

By symmetry, in tyrosine it is clear that the transition moment is situated in the plane either along the symmetry axis or 90° to it. We have used both for the calculation of the transfer efficiency and for the rotational anisotropies. Unfortunately, knowledge of transitional dipole moment is not complete, which can lead to major errors in the interpretation of energy transfer data if the wrong vectors are used and the motion is restricted. We have indications from the motional behavior of tyrosine fluorescence that the transition moment is along the short axis (Rigler et al., 1989).

The vector between both transition moments in tyrosine and tryptophan, for the energy transfer calculations (eq 3), was chosen from the center of all non-hydrogen atoms in the aromatic groups.

MD Simulation

(*a*) *Simulation Method.* The simulation method has been described elsewhere and is only briefly described below (MacKerell et al., 1988; Brooks et al., 1985). The simulations were performed on a Convex C210, and all other calculations were performed on a microVAX II.

Trx-S_2 and Trx-$(SH)_2$ both have been simulated starting from the 1.7-Å X-ray crystallographic structure of the Trx-S_2. The simulations were performed by using the CHARMM program (Brooks et al., 1983) with stochastic boundary conditions. The entire Trx molecule was placed in a 22-Å radius sphere of water of the TIP3P model (Jorgensen et al., 1983) centered around a point averaging the distances between Y70, Y49, W28, and W31 (x = 32.0 Å, y = 33.5 Å, and z = 5.0 Å in the coordinate set received from Hans Eklund). The position of the water sphere was selected so that all interesting regions (tyrosines, tryptophans, and the active center) were included in the water region. Atoms within 20 Å from the origin were propagated by using the Verlet algorithm (Verlet, 1967), and atoms outside the 20-Å radius were treated with Langevin dynamics with a friction constant of 50 ps^{-1} (Brooks et al., 1985). During the preparation of the system, the entire system was energy minimized for 200 steepest descent steps with harmonic constraints on the protein gradually decreased from 21 kcal/(mol $Å^2$) to 0 kcal/(mol $Å^2$) every 40 steps. The SHAKE routine (Ryckaert et al., 1977) was used to constrain all covalent bonds involving hydrogen atoms, allowing a time step of 2 fs. A nonbonded list cutoff at 9.0 Å was applied and updated every 10 steps. The electrostatic and van der Waals potentials were shifted to obtain a smooth transition to zero at 8.0 Å.

Initiation of the MD run was performed by instantaneously assigning all atoms a random velocity yielding an overall kinetic energy corresponding to 300 K. The temperature was checked every 20 fs (10 time steps) and allowed to vary ±10 K.

Coordinate sets were saved every 0.1 ps and used for further calculations. Each coordinate set was orientated for a minimum RMS difference of the backbone atoms compared to the X-ray coordinates of Trx-S_2 at 1.7-Å resolution; this was done to remove effects resulting from rotations of the water sphere in one direction and the protein in the opposite. The structure of Trx was simulated for 180 ps, of which the last 100 ps were used for the calculations.

(*b*) *Anisotropy Calculations.* From the trajectories, the motions of the tryptophan and tyrosine were studied and compared with results from fluorescence anisotropy measurements. These motions are related to the correlation function between the absorption, $\hat{\mu}_a$, and emission, $\hat{\mu}_e$, vectors of the aromatic rings as follows (Ehrenberg & Rigler, 1972):

$$r(t) = 0.4[e^{-(t/\theta_m)}]\langle P2[\hat{\mu}_a(0)\cdot\hat{\mu}_e(t)]\rangle \quad (5)$$

where $r(t)$ is the anisotropy as a function of time, θ_m is the rotational relaxation time for the overall rotation of the protein, $P2$ is the second-order Legendre polynomial, $P2(\alpha) = (3\alpha^2 - 1)/2$, and $\langle\,\rangle$ indicates a time average. In the simulations the overall rotation and translation of the protein are not present.

(*c*) *Energy Transfer Calculations.* The average rate of the energy transfer for the protein has been calculated pairwise for all tyrosine–tryptophan pairs, according to eq 7 (below). The dipole vectors were obtained from the last 100 ps of the simulations, as described above. These vectors were used to calculate the instantaneous value of κ^2/r^6 from which decay curves and average values were obtained. The decay curves were calculated as previously described (Henry & Hochstrasser, 1987):

$$I(t) = \left\langle \exp\left(-\int_0^t [k_t(\tau) + k_r]d\tau\right)\right\rangle \quad (6)$$

where $I(t)$ indicates the fluorescence intensity of the donor, $k_t(\tau)$ indicates the instantaneous energy transfer rate, and k_r is the intrinsic decay rate of the donor. The ensemble was chosen by successively choosing a point, every 100 fs, as starting point for the evaluation and evaluating the integral from this point with averaging over all time origins.

The mean efficiency of transfer was calculated from the κ^2/r^6 value averaged over the last 100 ps of the simulation using the following relations:

$$\langle k_\tau\rangle = (1.6 \times 10^7)\frac{1}{T}\int_0^T \frac{\kappa^2}{r^6}\,dt, \qquad T = 100 \text{ ps} \quad (7)$$

$$\text{Efficiency} = \frac{\langle k_\tau\rangle}{1 + \langle k_\tau\rangle} \quad (8)$$

the constant 1.6×10^7 was calculated from eq 2, obtained by Förster (1948).

Materials

E. coli thioredoxin (wt Trx) and the mutant thioredoxin with phenylalanine in position 31 (Trx-W28-W31F) were prepared as described earlier (Krause & Holmgren, 1991). The purity was checked by comparing the fluorescence with earlier fluorescence spectra. The protein was dissolved in a standard 50 mM pH 7.5 Tris buffer. The reduction was made by adding a 100-fold excess of DTT and ehecking the 3-fold increase in tryptophan emission. Absorption of oxidized DTT in the range 280–300 nm (Iyer & Klee, 1973) was found to be negligible in view of the quantum yield determinations. For the mutant, the reduction was checked by a 5-fold increase in fluorescence.

Time-Resolved Fluorescence Spectroscopy

Time-resolved fluorescence measurements were performed by using time-correlated single photon counting as previously described (Rigler et al., 1985; Claesens & Rigler, 1986). The experiments were performed at the MAX-synchrotron in Lund

(Rigler et al., 1987). At an excitation wavelength of 280 nm both tyrosine and tryptophan are excited, but at 300 nm only tryptophan is excited. The emission was monitored through a 295-nm linear filter with a bandwidth of 10 nm, for tyrosine studies, or through a cutoff filter at 345 nm for tryptophan studies. The pulse had typically a full-width half-maximum (FWHM) of 180 ps.

Data analysis was performed with a nonlinear parameterization procedure using the Marquardt algorithm (Marquardt, 1963). This also includes convolution of the model function with the measured excitation pulse. It was assumed that the fluorescence decay consisted of one or several exponential decays. The number of decay times was increased as long as the fit was improved as judged by the χ^2 value.

Anisotropy decays, $r(t)$, were calculated from the unpolarized intensity $I_m(t)$ and the perpendicularly polarized $I_\perp(t)$ fluorescence components by using

$$I_m(t) = \sum a_i e^{-K_i t} \tag{9a}$$

$$I_\perp(t) = g[\sum a_i e^{-K_i t}[1 - \sum_i r_i[e^{-(t/\rho_i)}]]] \tag{9b}$$

where r_i is the amplitude of the motion and ρ_i is the relaxation time of the motion. A correction factor (g) for the difference in detector sensitivity between the unpolarized and perpendicular polarized components, equal to 1.05, was used. If two rotation relaxation times are used it is assumed that

ρ_1 = rotational relaxation time of side chain

ρ_2 = rotational relaxation time of whole molecule

Here is it assumed that $\rho_1 \ll \rho_2$; the internal motion is much faster than the tumbling. If only one time is used in the fitting procedure, the relaxation time obtained is an average of both internal motion and overall tumbling with the longer time dominant. With three components, the fitting procedure did not converge.

Rotational relaxation times were fitted by assuming that each rotational decay is associated with all the fluorescence decays. We used 13 ns (500 channels) of the decay for the fits.

Decay Curves in the Presence of Energy Transfer

The fluorescence decay of the donor was assumed to be represented by one or several exponential decays, representing different conformations of the protein. To all of these exponential decays rates, a term due to energy transfer is added, yielding the following expression for the decay function of the donor:

$$I(t) = \sum_a \sum_b A \exp\left(-\int_0^t [k_d + k_\tau(\tau)]\, d\tau\right) \tag{10}$$

where a stands for all assumed configurations and b stands for all donor–acceptor pairs, k_d is the natural decay rate in the absence of any transfer, k_τ is the transfer rate for that specific pair, and A is the amplitude. In a steady-state model, k_τ would be constant in time, but from the dynamic study we use the instantaneous rate of k_τ described above as a function of time.

If the natural decay of the donor and the acceptor consists of one or several exponential decays, the decay of the acceptor in the presence of the donor will be described by

$$I(t) = \sum_a a e^{-\int K_a dt} + \sum_b b[e^{-\int [(K_\tau(t)+K_d)]dt} - e^{-\int (K_a dt)}] \tag{11}$$

where a is the component occurring from the directly excited acceptor and b is the portion due to the acceptors that have been excited by energy transfer.

Measurement of Energy Transfer

The measurement of the energy transfer from tyrosine to tryptophan is not straightforward as there is no wavelength where one can excite tyrosine but not tryptophan. There are several methods to perform these measurements:

(A) The relative quantum yield of tryptophan emission when excited in the wavelengths from 260 to 310 nm (Saito et al., 1980) can be compared with theoretically calculated curves for different energy transfer efficiencies, obtained from tyrosine and tryptophan absorption spectra in solution. This method requires that the tryptophan population in the protein has the same spectral properties as tryptophan free in solution, but it may have another quantum yield, as the theoretically calculated curves are calculated from the absorption spectrums from tyrosine and tryptophan.

(B) The decay rate of the donor should be different in the absence and presence of an acceptor. From other studies (Rigler et al., 1989), we know the normal decay rate for tyrosine in its hydrogen-bonded form and in its free form. If tyrosine fluorescence in Trx decays faster, it is an indication for the existence of energy transfer.

(C) Another possible way to measure the energy transfer rate is by recording the tryptophan decay at 300 and 280 nm (see above eq 11).

Results

Steady-State Fluorescence

Fluorescence Intensity. The increase in tryptophan fluorescence intensity in wt Trx-S_2 on reduction remained in the mutant Trx-W28-W31F and was 5-fold compared to 3-fold in wt. This demonstrates that W28 was the source of the increase and indicates that W31 is highly quenched along with W28 in the oxidized form, as previously found (Krause & Holmgren, 1991).

Tryptophan Picosecond Fluorescence

(*a*) *Tryptophan Lifetimes When Excited at 300 nm.* Three major lifetimes (0.1, 0.3, and 1.0 ns) existed in wt Trx-S_2 along with one less populated form (5.0 ns). In wt Trx-$(SH)_2$ the fast 0.1-ns component in the lifetime spectrum had disappeared (Table Ia). The mutant Trx-W28-W31F had similar features as the wild-type, and the disappearance of the fastest lifetime upon reduction still existed. Furthermore, in Trx-W28-W31F the population of the 0.3-ns component was strongly decreased. In the mutant thioredoxin, the longest decay time was longer than in the wt protein.

(*b*) *Tryptophan Lifetimes When Excited at 280 nm.* When fluorescence in wt Trx is excited at 280 nm, both tyrosine and tryptophan emission occur, but by using a cutoff filter at 345 nm only the fluorescence emission from tryptophan is observed (Table Ib). Emission can occur either from direct excitation of tryptophan or by transfer of energy from an excited tyrosine to tryptophan as described above (eq 11). We tried to use this equation and fit it simultaneously to tryptophan fluorescence excited at both 280 and 300 nm. However, this gave no reproducible results, apparently due to the transfer of energy to tryptophan being too small relative to the direct excitation. Instead, we applied sums of exponential decay functions to the tryptophan fluorescence excited at 280 nm; these function gave more reproducible results, although the fits were not that good ($\chi^2 > 1.60$).

Some changes in the lifetime spectra after excitation at 280 nm, as compared to the 300 nm spectra, are noticeable. In the wt Trx-S_2, the population of the fast component was increased, whereas in wt Trx-$(SH)_2$ the lifetime distributions

Table I: Fluorescence Decay of Tryptophan Fluorescence in Thioredoxin

sample	ex wave-length	decay time (ns)[a]	rel amp[a]	χ^2
(a) Trx-W28-W31-S_2[b]	300 nm	5.1 ± 0.66	0.004 ± 0.001	1.78
		1.0 ± 0.04	0.16 ± 0.01	
		0.33 ± 0.02	0.63 ± 0.05	
		0.10 ± 0.05	0.21 ± 0.04	
Trx-W28-W31-$(SH)_2$	300 nm	3.5 ± 0.25	0.09 ± 0.02	1.39
		1.6 ± 0.08	0.40 ± 0.01	
		0.36 ± 0.02	0.50 ± 0.02	
Trx-W28-W31F-S_2	300 nm	7.3 ± 0.54	0.05 ± 0.01	1.50
		1.8 ± 0.27	0.07 ± 0.005	
		0.33 ± 0.13	0.31 ± 0.44	
		0.19 ± 0.05	0.57 ● 0.44	
Trx-W28-W31F-$(SH)_2$	300 nm	5.7 ± 0.41	0.16 ● 0.02	1.47
		1.9 ± 0.11	0.44 ± 0.01	
		0.35 ± 0.03	0.40 ± 0.02	
(b) Trx-W28-W31-S_2	280 nm	2.7 ± 0.38	0.01 ± 0.005	2.10
		1.1 ± 0.04	0.14 ± 0.006	
		0.31 ± 0.01	0.41 ± 0.02	
		0.07 ± 0.01	0.45 ± 0.06	
Trx-W28-W31-$(SH)_2$	280 nm	3.5 ± 0.39	0.07 ± 0.03	1.59
		1.7 ± 0.09	0.36 ± 0.02	
		0.30 ± 0.01	0.57 ● 0.01	
Trx-W28-W31F-S_2	280 nm	7.1 ± 0.45	0.05 ± 0.005	1.71
		1.8 ± 0.17	0.09 ± 0.003	
		0.28 ± 0.03	0.49 ± 0.13	
		0.10 ± 0.05	0.37 ± 0.07	
Trx-W28-W31F-$(SH)_2$	280 nm	5.8 ± 0.56	0.16 ± 0.03	1.63
		2.1 ± 0.13	0.47 ± 0.02	
		0.30 ± 0.03	0.37 ± 0.02	

[a] Errors are for a 95% confidence interval. [b] wt Trx here shown with the tryptophan fluorophores.

Table II: Rotational Relaxation Times for Tryptophan Emission in Trx

sample	ex wave-length	relax time (ρ) (ns)[a]	r_0[a]	χ^2
		Two Relaxation Times		
Trx-W28-W31-S_2	300 nm	3.7 ± 0.28	0.25 ± 0.004	1.07
		0.01 ± 0.01	0.23 ± 0.11	
Trx-W28-W31-$(SH)_2$	300 nm	4.8 ± 0.20	0.25 ± 0.003	0.96
		0.02 ± 0.02	0.16 ● 0.13	
Trx-W28-W31F-S_2	300 nm	9.3 ● 0.79	0.19 ± 0.007	1.05
		0.31 ± 0.07	0.10 ● 0.008	
Trx-W28-W31F-$(SH)_2$	300 nm	5.8 ± 0.25	0.25 ± 0.004	0.98
		0.12 ± 0.11	0.04 ± 0.02	
Trx-W28-W31-S_2	280 nm	2.6 ± 0.27	0.16 ± 0.006	1.05
		0.05 ± 0.03	0.09 ± 0.03	
Trx-W28-W31-$(SH)_2$	280 nm	4.9 ± 0.35	0.16 ± 0.004	1.03
		0.02 ± 0.02	0.17 ± 0.12	
Trx-W28-W31F-S_2	280 nm	11.1 ± 1.53	0.12 ± 0.005	1.11
		0.23 ± 0.05	0.11 ± 0.01	
Trx-W28-W31F-$(SH)_2$	280 nm	6.2 ± 0.48	0.16 ± 0.005	1.10
		0.15 ± 0.07	0.07 ± 0.02	
		One Relaxation Time		
Trx-W28-W31-S_2	300 nm	3.5 ± 0.23	0.26 ± 0.003	1.05
Trx-W28-W31-$(SH)_2$	300 nm	4.8 ± 0.20	0.25 ± 0.003	0.96
Trx-W28-W31F-S_2	300 nm	6.4 ± 0.24	0.23 ± 0.002	1.48
Trx-W28-W31F-$(SH)_2$	300 nm	5.7 ± 0.20	0.25 ± 0.003	1.10
Trx-W28-W31-S_2	280 nm	2.3 ± 0.16	0.17 ± 0.003	1.13
Trx-W28-W31-$(SH)_2$	280 nm	4.8 ± 0.32	0.16 ● 0.003	1.03
Trx-W28-W31F-S_2	280 nm	6.6 ± 0.41	0.15 ± 0.002	1.48
Trx-W28-W31F-$(SH)_2$	280 nm	5.8 ± 0.34	0.17 ± 0.003	1.12

[a] Errors are for a 95% confidence interval.

at 280 and 300 nm were similar. In the mutant Trx-W28-W31F, the lifetime spectrum was more similar to the spectrum after excitation at 300 nm (Table I). Here too, the fits were not as good as with an excitation wavelength of 300 nm.

(*c*) *Anisotropy of Tryptophan Fluorescence.* We could identify two types of fast internal motions in the thioredoxin: one very fast relaxation time in the range of 10 ps and one fast in the range of 200 ps (Table II). The very fast component had an initial r_0 of approximately 0.2, but poorly determined, while the fast had an initial r_0 around 0.1. The very

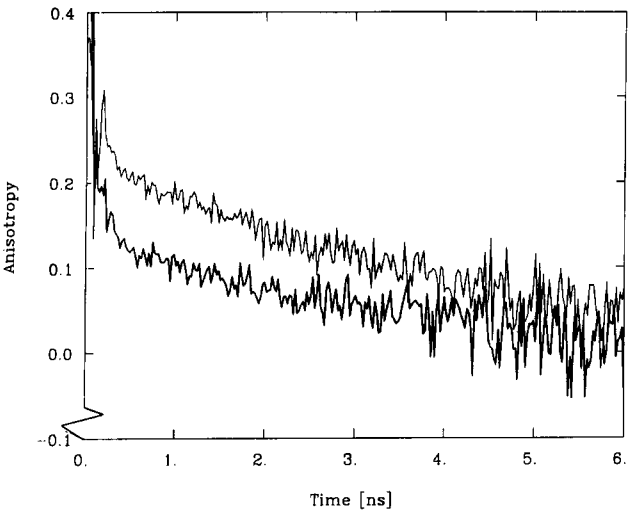

FIGURE 2: Comparison of anisotropy of Trx-W28-W31-$(SH)_2$ excited at 280 nm (thick line) and 300 nm (thin line). Observe the lower amplitude when 280 nm is used as excitation wavelength.

Table III: Fluorescence Decay of Tyrosine Fluorescence in Thioredoxin

sample	ex wave-length	decay time (ns)[a]	rel amp[a]	χ^2
Trx-W28-W31-S_2	280 nm	1.2 ± 0.01	0.33 ± 0.01	1.15
		0.23 ± 0.01	0.67 ± 0.03	
Trx-W28-W31-$(SH)_2$	280 nm	3.3 ± 0.76	0.03 ± 0.02	1.18
		1.4 ± 0.13	0.27 ± 0.03	
		0.3 ± 0.02	0.70 ± 0.02	
Trx-W28-W31F-S_2	280 nm	4.1 ± 0.70	0.03 ± 0.01	0.98
		1.4 ± 0.06	0.34 ± 0.01	
		0.27 ± 0.01	0.63 ± 0.01	
Trx-W28-W31F-$(SH)_2$	280 nm	5.8 ± 1.17	0.05 ± 0.02	1.02
		1.7 ± 0.14	0.36 ± 0.01	
		0.33 ± 0.02	0.59 ± 0.02	

[a] Errors are for a 95% confidence interval.

fast relaxation time could only be observed when the fast one was not present and might occur from the tryptophan as well as being an artifact of the fitting procedure or arise from scattered light. The fast relaxation time (120–310 ps) occurred in Trx-W28-W31F, and the very fast (10–50 ps) was detected in wt Trx (Table II).

Overall tumbling of the molecule is shown both by a long decay time, when two rotational motions were assumed, as well as by the decay time when only one rotational relaxation time was fitted. In wt Trx-S_2 the long relaxation time was much faster than in all other cases, 2 ns compared to 5–9 ns. When fluorescence was measured following excition at 280 nm, the amplitude of the overall tumbling decreased from around 0.25 to 0.17 (Figure 2).

In Trx-W28-W31F-S_2, the r_0 for the long relaxation time was lower when two rotational times were fitted, as compared to the other cases, and the fast relaxation time in Trx-W28-W31F-$(SH)_2$ had a smaller amplitude than the others.

Tyrosine Picosecond Fluorescence

(*a*) *Decay Times for Tyrosine 49/70.* The tyrosine decay was well fitted by two or three exponential decays, with the long time of approximately 3 ns only populated by a few percent of the population (Table III). This long time was not observed in wt Trx-S_2. The middle time (1 ns) accounted for 30% of the population and the fast decay (0.3 ns) consisted of 70%. In Trx-W28-W31F the fast and the middle decay times were approximately 10–20% longer than in wt Trx (Table III).

Table IV: Rotational Relaxation Times for Tyrosine Emission in Trx

sample	ex wave-length	relax time (ρ) (ns)[a]	amp r_0[a]	χ^2
	Two Relaxation Times			
Trx-W28-W31-S_2	280 nm	10.2 ± 5.7	0.21 ± 0.02	0.87
		0.30 ± 0.27	0.07 ± 0.02	
Trx-W28-W31-$(SH)_2$	280 nm	6.0 ± 0.92	0.23 ± 0.01	1.14
		0.01 ± 0.08	0.22 ± 0.82	
Trx-W28-W31F-S_2	280 nm	6.8 ± 1.13	0.23 ± 0.01	0.94
		0.21 ± 0.30	0.04 ± 0.02	
Trx-W28-W31F-$(SH)_2$	280 nm	5.9 ± 0.73	0.22 ± 0.01	1.00
		0.02 ± 0.04	0.34 ± 0.52	
	One Relaxation Time			
Trx-W28-W31-S_2	280 nm	6.1 ± 1.0	0.24 ± 0.006	0.91
Trx-W28-W31-$(SH)_2$	280 nm	5.6 ± 0.74	0.23 ± 0.006	1.07
Trx-W28-W31F-S_2	280 nm	6.0 ± 0.60	0.24 ± 0.005	0.93
Trx-W28-W31F-$(SH)_2$	280 nm	5.7 ± 0.65	0.22 ± 0.007	1.03

[a] Errors are for 95% confidence interval.

(*b*) *Anisotropy of Tyrosines.* As with tryptophan emission, we could separate two cases: one with a very fast component (10–20 ps) and a higher total amplitude (0.4–0.5) and one with a fast component (200–300 ps) and a lower amplitude of (0.27–0.28). The very fast component occurred in the Trx-$(SH)_2$ form both in the mutant and in the wild-type, and the fast component occurred in Trx-S_2 (Table IV).

The overall tumbling relaxation time was constant in all experiments (5.6–6.1 ns) when one relaxation time was fitted to the data. If two relaxation times were used, the overall tumbling rate could only be determined with large error bars.

Molecular Dynamics

(*a*) *Motion of Aromatic Residues.* The correlation functions of all four aromatic side chains are shown in Figures 3 and 4. All correlation functions consisted of a very fast (a few picosecond) decay followed by a second phase. This second phase consisted either of a slower decay or of reaching a plateau value.

Tyrosine 49 was located in a fixed position (Katti et al., 1990), by a hydrogen bond to asparagine 104 during the last 100 ps in both simulations. The motional space was thus limited in Trx-$(SH)_2$, while in Trx-S_2 the motion was somewhat less restricted for rotation around the long axis (Figure 3). Exactly the same behavior could be seen for Y70 (Figure 3), although it was in an exposed position on the protein surface (Figure 1).

The motion of W28 was very restricted both in Trx-S_2 and Trx-$(SH)_2$, while W31 appeared much more flexible and showed an increase in mobility in the oxidized form (Figure 4).

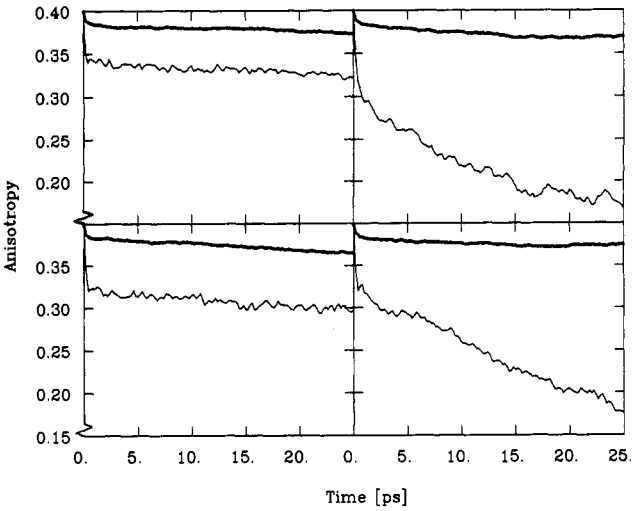

FIGURE 3: *P2* correlation function of Y49 (lower curves) and Y70 (upper curves) in Trx-S_2 (left curves) and Trx-$(SH)_2$ (right curves) from molecular dynamics simulations. The thick line is from the symmetry axis and the thin line from the short axis.

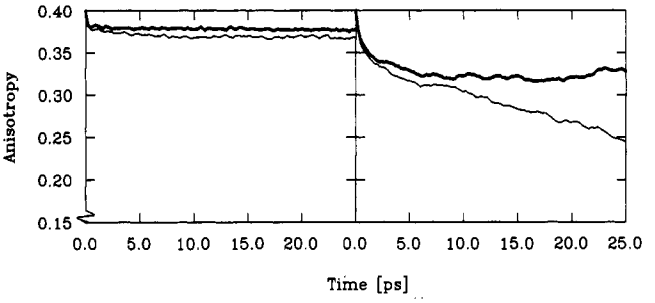

FIGURE 4: *P2* correlation function of W28 (left curves) and W31 (right curves) from molecular dynamics simulations. The thick line is from Trx-S_2 and the thin line from Trx-$(SH)_2$.

(*b*) *Energy Transfer.* The results from the calculations of energy transfer are given in Table V. If we assume the transition moment in tyrosine to be along the short axis, we see that Y49 can not contribute to any major energy transfer. We have between 0% and 7% energy transfer to W28 and W31. This low energy transfer rate is due to both distance (20 and 28 Å) and low κ^2 values (Figure 1). The energy transfer from Y70 is about 50% to W28 in the Trx-S_2 X-ray structure and in the Trx-S_2 simulation compared with 38%

Table V: Energy Transfer Rate, Values of κ^2, and Distance between All Tyrosine–Tryptophan Pairs

coordinate set	Trx-$(SH)_2$[b] eff	κ^2	dist	Trx-S_2[c] eff	κ^2	dist	Trx-S_2 X-ray coor[d] eff	κ^2	dist
				Transfer between All Tyrosine–Tryptophan Pairs					
Y70-W28 cg-cz	3%	0.04	16.7	4%	0.05	16.5	5%	0.01	17.2
Y70-W28 cd1-cd2	38%	0.84		52%	0.98		53%	1.07	
Y70-W31 cg-cz	11%	0.43	19.5	10%	0.44	20.2	8%	0.26	19.2
Y70-W31 cd1-cd2	24%	1.02		16%	0.76		19%	0.24	
Y49-W28 cg-cz	10%	0.49	20.6	16%	0.77	20.0	8%	0.36	20.3
Y49-W28 cd1-cd2	4%	0.18		2%	0.24		7%	0.65	
Y49-W31 cg-cz	2%	0.82	29.4	2%	0.74	28.4	3%	0.96	28.0
Y49-W31 cd1-cd2	1%	0.26		2%	1.17		0%	0.09	
				Total Transfer Rate from Each Tyrosine					
Y70 cg-cz	14%			23%			13%		
Y70 cd1-cd2	53%			60%			62%		
Y49 cg-cz	13%			18%			11%		
Y49 cd1-cd2	5%			4%			7%		

[a] eff, the percentage of the tyrosine population that is transferred to the tryptophan; κ^2, the value of κ^2 (eq 3) between the tyrosine and the tryptophan involved in the transfer; dist, the distance between the tyrosine and tryptophan involved in the transfer. [b] Calculated from the simulation of Trx-$(SH)_2$. [c] Calculated from the simulation of Trx-S_2. [d] Calculated from the minimized X-ray structure of Trx-S_2 (Katti et al., 1990).

in the Trx-$(SH)_2$ simulation. This effect is compensated by the energy transfer to W31 that is 24% in Trx-$(SH)_2$ and only 16–19% in Trx-S_2. The distance difference between Trx-$(SH)_2$ and Trx-S_2 is hardly affecting the transfer rate at all, compared to differences in κ^2. The total energy transfer rates in Trx-S_2 and Trx-$(SH)_2$ hardly differ.

It is evident that there is a strong dependence on the choice of emission dipole direction for tyrosine. If we assume the dipole to be along the long axis, the energy transfer from Y70 to both W31 and W28 will be lower due to unfavorable orientation of the tryptophans with respect to Y70. We will have low κ^2 values (0.04–0.43). With the long axis, the energy transfer from Y49 and W28 will be facilitated compared to the short axis by a higher κ^2 value. The difference between the X-ray coordinates and the Trx-S_2 simulation is quite small when one examines the transfer rates, while κ^2 value differs dramatically in some transfer pairs.

Discussion

Measurements of Energy Transfer

We show below that there are no major changes in energy transfer rate between wt Trx and Trx-W28-W31F or between Trx-$(SH)_2$ and Trx-S_2. We have used several methods for measuring the internal energy transfer from tyrosine to tryptophan; they all have some advantages and disadvantages as discussed below.

(*a*) *Steady State.* The simplest method is to measure the relative quantum yield in the range between 260 and 310 nm for the tyrosine–tryptophan pair (Saito, 1980). Results obtained from Trx with this method showed an energy transfer from tryptophan to tyrosine (data not shown). The explanation for this is that W28 and/or W31 have different spectral properties compared with tryptophan in solution. This is not surprising as W31 is almost totally quenched and W28 also is strongly quenched. Thus we could obtain little information from these measurements.

(*b*) *Tyrosine Decay.* The transfer efficiency can be calculated from the difference in the tyrosine decay rate in the presence and absence of tryptophan. This measurement can be performed when a mutant with both tryptophans exchanged for another nonfluorescent residue will become available.

The decay rate in Trx-W28-W31F was approximately 10–20% slower than in wt Trx, indicating that there is some energy transfer to W31 that makes the tyrosine decay faster when W31 is present. We will discuss the consistency of this with the molecular dynamics simulation below.

One explanation for the two fluorescence decay times seen in tyrosine (Table III) is that tyrosine decays with two different rates if hydrogen bonded or not bonded (Rigler et al., 1989). When tyrosine is hydrogen bonded, the decay time is approximately 0.5 ns, and when not bonded, it is 3.0 ns. The two populations that decay with rates of 1.5 and 0.3 ns (Table III) would then represent two forms of tyrosine: one that is hydrogen bonded and one that is not. These populations would then both transfer with an efficiency of about 50%. Also there are other explanations for the splitting of the tyrosine decay in two decay rates, we prefer the present explanation as it is consistent with the results from the MD simulations.

We know from the structure of Trx-S_2 that Y49 can have only a small energy transfer rate, due to the long distance to a tryptophan. From the molecular dynamics simulations, we could see that Y49 has a tendency to be hydrogen bonded to D104, indicating that the short tyrosine lifetime would arise from Y49 and the long lifetime from Y70. As the decay rates were almost constant in Trx-$(SH)_2$ and Trx-S_2, there seems not to be any change in the energy transfer rate on reduction.

(*c*) *Tryptophan Time-Dependent Fluorescence.* By measuring the decay of the tryptophan emission when excited at both 280 and 300 nm, it should be possible to simultaneously fit these measurements to eq 11. This assumes that the lifetime distribution for tryptophan is the same when excited at 280 and 300 nm. We could not fit the measurements satisfactorily to eq 11 ($\chi^2 > 4.0$), and the parameters were not well determined. This can be explained by different lifetime populations with excitation wavelengths of 280 and 300 nm. Thus this method gave no further information. It is not surprising that the lifetime distribution is different after excitation at 280 nm compared to 300 nm as different amounts of L_a and L_b are involved in the fluorescence process (Ruggiero et al., 1990).

The bad fits obtained by fitting only by a sum of exponential decays to the tryptophan fluorescence after excitation at 280 nm indicates that the decay function can not be completely described by negative exponential functions and might be an effect of energy transfer. We performed several different fitting methods, both using negative amplitudes and a globular fitting method to eq 11.

Simulation of Energy Transfer Rates

Do we get a more accurate value of energy transfer rates if we perform a simulation compared with using the X-ray coordinates? Can we assume κ^2 equal to $^2/_3$?

These are two of the questions we wanted to answer by the simulations. If we assume that the transition moment of tyrosine is along the short axis, κ^2 for transfer from Y70 is slightly higher than $^2/_3$ in all transfer pairs, whereas, for Y49, κ^2 for some transfer pairs are a factor of three lower than $^2/_3$. Thus the assumption that κ^2 equals $^2/_3$ is hardly valid for aromatic side chains in a globular protein (Table V).

If we would have calculated the transfer rates from the X-ray structure, we would have obtained κ^2 values that in some cases differ by a factor of higher than 10 from the corresponding average value from the simulation (Table V). This indicates that the use of a MD simulation probably spans the motional space for the dipoles, giving a better value of κ^2.

Energy Transfer Rates

From the measurements, we could conclude that there are no major changes in energy transfer rate between Trx-S_2 and Trx-$(SH)_2$, while there was a slight increase in energy transfer rate from wt Trx compared with the mutant Trx-W28-W31F. This is consistent with the simulations if the transition moment in tyrosine is assumed to be the short axis (Table V).

The simulations showed that we have roughly a 50% energy transfer efficiency from Y70 to W28 and roughly 20% from Y70 to W31 if we assume that the transition moment in tyrosine is along the short axis. We can also notice that we would have got the same energy transfer rate if we would have used the X-ray coordinates for the calculation. We can also make the assumption that Y70 is not hydrogen bonded and then would have a lifetime without transfer of approximately 3 ns. Some simple calculations indicate that the middle component of tyrosine fluorescence decay would be 1.33 ns in wt Trx, 1.5 ns in Trx-W28-W31F, and in good agreement with the measurements (Table III).

Fluorescence Lifetimes

(*a*) *Lifetimes at 300 nm.* We can reproduce the major features that were shown by Merola et al. (1988) for thioredoxin fluorescence. Of five lifetimes found previously in Trx-S_2 and four in Trx-$(SH)_2$, we could only find four and three, respectively. This may be explained by a shorter pulse width from the laser equipment used previously compared with

the present synchrotron source. Another limitation in our measurements is data collection time, whereas the laser is stable for many hours, the synchrotron loses most of it intensity in 2 h (Rigler et al., 1987).

The fluorescence from Trx-W28-W31F had the same features as from wt Trx. Both showed with the disappearance of a fast lifetime and the population changes, evidence of the almost total quenching of W31 fluorescence. Apparently W28 is in a similar environment in both wt Trx and Trx-W28-W31F. However, there are some small differences between the fluorescence decays that we believe are relevant for analysis of the fluorescence from W31. The long relaxation time in wt Trx is much shorter than in Trx-W28-W31F, indicating that this relaxation has two components, a long component from W28 and one shorter one from W31. We cannot separate these lifetimes in our fitting procedure. In Trx-W28-W31F the 0.3 ns component was less populated than in wt Trx, suggesting that W31 fluorescence consists of a 0.3 ns and a 3.0 ns lifetime component.

The lifetimes in wt Trx are slightly shorter than in Trx-W28-W31F (Table I), indicating that W28 might be quenched by internal energy transfer from W28 to W31. This energy transfer is not possible from W28 to F31.

(*b*) *Lifetimes at 280 nm.* All major features were retained as the excitation wavelength was changed from 300 to 280 nm. The main difference compared with the 300-nm measurements was the fact that χ^2 was higher. This may be due to the transfer contribution (the *b* population in eq 11). The fast population (decay time of 100 ps) in wt Trx-S_2 occupied 45% when the excitation wavelength was 280 nm and only 21% when 300 nm was used. This could be explained if energy transfer is easier to the 100-ps population than to the 300-ps population. However, this behavior could not be seen in Trx-W28-W31F. It is tempting to speculate that the W31 residue has a 300-ps component not involved in energy transfer. Thus the 300-ps component was decreased with excitation at 280 nm in comparison to the 100-ps component, which appears from W28.

Anisotropy

(*a*) *Internal Motion of Tryptophan and Tyrosine.* From the time-resolved anisotropy measurements of tyrosine and tryptophan measurements, we can separate three different rotational correlation times even if in some cases they could not statistically be separated from each other (Tables II and IV). We detected a very fast internal motion (10–20 ps) in the tryptophan emission of wt Trx and in the tyrosine motion of Trx-$(SH)_2$. This decay time was poorly determined due to the very fast decay and due to the fact that one channel in this study corresponds to 21 ps. When a fast internal motion (100–300 ps) can be seen, the very fast component can not be detected. The third component had a long correlation time (nanoseconds). The very fast time occurs from nonmotional relaxation, very fast vibrations of a side chain, scattered light, or might be an artifact of the fitting procedure. The fast time occurs from internal motion of the side chain, and the long time occurs from tumbling of the whole protein.

The *P*2 correlation functions calculated from the molecular dynamics simulations can be separated into two parts, a very fast relaxation (picoseconds) and a second phase. The very fast phase occurs from vibrations of the side chain. The second phase either relaxes to a plateau value (tyrosine decay in Trx-S_2 and W28 fluorescence) or shows a decay rate of approximately 100 ps. When the plateau value is reached, the motion of the side chain will be restricted to vibrations, but when a decay occurs, the side chain undergoes rearrangements, with respect to the remainder of the protein.

The measurements and the molecular dynamics simulation are consistent if we assume that the transition moment in tyrosine is along the short axis. The motion seen from the simulations of W28 is restricted both in Trx-$(SH)_2$ and Trx-S_2, while W31 shows an internal mobility (Figure 4). This is consistent with the measurements where no internal mobility could be seen in wt Trx-S_2 and wt Trx-$(SH)_2$ and the fact that W31 is highly quenched (Table II). The mutant Trx-W28-W31F had increased mobility of W28, indicating that we have a more flexible active site in Trx-W28-W31F than in wt Trx. The motions of Y49 and Y70 are restricted in Trx-S_2 as shown by the simulation (Figure 2) and by the measurements (Table IV), while in Trx-$(SH)_2$ an internal motion could be seen. Thus the reduction of Trx-S_2 makes the structure more flexible, giving Y49 and Y70 more space to move within.

When tryptophan was excited at 280 nm more of the fluorescence occurs from the L_b transition moment (Ruggiero et al., 1990). This explains that the amplitude of the long rotational relaxation time of tryptophan fluorescence when excited at 280 nm was lower than when excited at 300 nm.

(*b*) *The Overall Tumbling of Trx.* In all samples an overall tumbling can be seen with a correlation time of about 5 ns, even if some significant differences occur in the tryptophan measurements. It is interesting to see that we could make exact measurements of the overall tumbling rate by measuring tyrosine fluorescence in the presence of tryptophan; this makes it possible to use two different methods to determine the overall tumbling rates of proteins.

The overall tumbling of wt Trx-S_2, as seen by tryptophan emission with an excitation wavelength of 280 nm, was much faster than for all other measurements. Even when an excitation wavelength of 300 nm is used the tumbling of wt Trx-S_2 was faster than in the other samples, indicating that the motion behavior is more complicated than the simple "overall ↔ internal motion" model that we have applied. This is also exemplified by the amplitude of the overall tumbling of Trx-W28-W31F-S_2 being lower than in the other studies.

(*c*) *Dipole Moment in Tyrosine.* We do not know the direction of the transition moment in tyrosine. The consistency of increased mobility upon reduction between simulations, assuming a short axis moment, and tyrosine anisotropy are strong indications for the short axis. Earlier studies of tyrosine anisotropy in the absence of tryptophan (Rigler et al., 1989) show an internal motion of tyrosine that most likely is consistent with the transition moment along the short axis.

(*d*) *Mobility Changes of Tyrosine with Reduction.* How is the protein structure influenced by the breaking of the disulfide bond? As shown by Dyson et al. (1990), the only significant structural changes are around the active site. Can there be any other important changes that not were detected by NMR? We show both from the simulations and from the measurements of tyrosine fluorescence that both Y49 and Y70 have an increased motional space for rotation around their long axis. This increased rotation might give rise to sharper peaks for the protons in Y49 and Y70. However, to our knowledge this has not yet been analyzed.

In the reduced protein, we can detect a mobility change of tyrosine but not of W28 (Tables II and IV), indicating that the whole structure becomes looser with reduction but that W28 still is fixed. This was also shown from the MD simulations (Figures 3–4).

(*e*) *Mobility Changes of Tryptophan and Not of Tyrosine upon Mutation.* With the mutation of W31 to F31, the mobility of W28 changes so a fast decay time occurs. The mu-

tation also makes the very fast decay rate unobservable. The mobilities of Y49 and Y70 were not changed, indicating that the mutation only disturbed the mobility close to the active site. The structure around W28 can not be significantly changed since the lifetime distribution is very similar in wt Trx and Trx-W28-W31F.

CONCLUSIONS

Mutating W31 in wt Trx to phenylalanine (Trx-W28-W31F) made the motion of W28 less restricted, without large-scale changes in the surrounding of W28 as judged by lifetime distribution. The structure of the active site cannot be highly changed since the activity is retained and the lifetime distribution of W28 was unchanged. The motion of the rest of the protein was not significantly affected with this mutation.

When we reduced Trx-S_2 to Trx-$(SH)_2$, we could observe an increased motion of Y49 and Y70, which are both situated far away from the active-site disulfide bond, but not of W28, which is situated close to the disulfide bridge. Thus the reduction seems to make the whole structure looser, giving rise to an increased motional space for Y70 and Y49.

We show that, if we assume that the transition moment in tyrosine is along the short axis, the motions of tyrosine examined by correlation functions from the simulations were consistent with the measurements.

There is energy transfer from tyrosine to tryptophan in thioredoxin. The results from these measurement were consistent with results from the simulations, giving approximately 50% transfer from Y70 to W28 and 20% from Y70 to W31. The fluorescence from W28 seems to be quenched by energy transfer to W31.

ACKNOWLEDGMENTS

We thank R. Jakabffy for technical assistance and Prof. H. Eklund for the X-ray coordinates.

Registry No. Tryptophan, 73-22-3; tyrosine, 60-18-4.

REFERENCES

Brooks, B. R., Bruccoleri, R. E., Olafson, B. D., States, D. J., Swaminathan, S., & Karplus, M. (1983) *J. Comput. Chem. 4*, 187–217.

Brooks, C. L., Brunger, A., & Karplus, M. (1985) *Biopolymers 24*, 843–865.

Claesens, F., & Rigler, R. (1986) *Eur. Biophys. J. 13*, 331–342.

Dyson, H. J., Gippert, G. P., Case, D. A., Holmgren, A., & Wright, P. E. (1990) *Biochemistry 29*, 4129–4136.

Ehrenberg, M., & Rigler, R. (1972) *Chem. Phys. Lett. 14*, 539–544.

Förster, T. H. (1948) *Ann. Phys. (Leipzig) 6 (2)*, 55–75.

Henry, E. R., & Hochstrasser, R. M. (1987) *Proc. Natl. Acad. Sci. U.S.A. 84*, 6142–6146.

Holmgren, A. (1972) *J. Biol. Chem. 247*, 1992–1998.

Holmgren, A. (1981) *Biochemistry 20*, 3204–3207.

Holmgren, A. (1985) *Annu. Rev. Biochem. 54*, 237–271.

Iyer, K. S., & Klee, W. A. (1973) *J. Biol. Chem. 248*, 707–710.

Jorgensen, W. L., Chandrasekar, J., Madura, J. D., Impey, R. W., & Klein, M. L. (1983) *J. Chem. Phys. 79*, 926.

Katti, S., LeMaster, D. M., & Eklund, H. (1990) *J. Mol. Biol. 212*, 167–184.

Krause, G., & Holmgren, A. (1991) *J. Biol. Chem. 266*, 4056–4066.

Lakowicz, J. R. (1983) in *Principles of Fluorescence Spectroscopy*, pp 303–379, Plenum Press, New York.

MacKerell, A. D., Nilsson, L., Rigler, R., & Saenger, W. (1988) *Biochemistry 27*, 4547.

Marquardt, D. W. (1963) *J. Soc. Ind. Appl. Math. 11*, 431–444.

Merola, F., Rigler, R., Holmgren, A., & Brochon, J. C. (1989) *Biochemistry 28*, 3383–3398.

Rigler, R., Claesens, F., & Kristensen, O. (1985) *Anal. Instrum. (N.Y.) 14*, 525–546.

Rigler, R., Kristensen, O., Roslund, J., Thyberg, P., Oba, K., & Eriksson, M. (1987) *Phys. Scr. T17*, 204–208.

Rigler, R., Roslund, J., & Forsen, S. (1989) *Eur. J. Biochem. 188*, 541–545.

Ruggiero, A. J., Davidson, C. T., & Fleming, G. R. (1990) *J. Am. Chem. Soc. 112*, 1003–1014.

Ryckaert, J. P., Ciccotti, G. & Berendsen, H. J. C. (1977) *J. Comput. Phys. 23*, 327–337.

Saito, Y., Tachibana, H., Hayashi, H., & Wada, A. (1980) *Photochem. Photobiol. 33*, 289–295.

Verlet, L. (1967) *Phys. Rev. 159*, 98–105.

Yamamoto, Y., & Tanaka, J. (1972) *Bull. Chem. Soc. Jpn. 45*, 1362.